

**This is the preprint of the contribution published as:**

**Löffler, M., Schrader, M., Lüders, K., Werban, U., Hornbruch, G., Dahmke, A., Vogt, C., Richnow, H.H.** (2022):

Stable hydrogen isotope fractionation of hydrogen in a field injection experiment: Simulation of a gaseous H<sub>2</sub> leakage

*ACS Earth Space Chem.* **6** (3), 631 - 641

**The publisher's version is available at:**

<http://dx.doi.org/10.1021/acsearthspacechem.1c00254>

# Stable Hydrogen Isotope Fractionation of Hydrogen in a Field Injection Experiment: Simulation of a gaseous H<sub>2</sub> Leakage

Michaela Löffler<sup>1</sup>, Merle Schrader<sup>1</sup>, Klas Lüders<sup>2</sup>, Ulrike Werban<sup>3</sup>, Götz Hornbruch<sup>2</sup>, Andreas Dahmke<sup>2</sup>, Carsten Vogt<sup>1,\*</sup>, Hans H. Richnow<sup>1</sup>

5 <sup>1</sup> Department of Isotope Biogeochemistry, Helmholtz Centre for Environmental Research –UFZ, Leipzig 04318, Germany

<sup>2</sup> Aquatic Geochemistry & Hydrogeology, Applied Geosciences, University of Kiel, Kiel 24118, Germany

<sup>3</sup> Department of Monitoring and Exploration Technologies, Helmholtz Centre for Environmental Research –UFZ, Leipzig 04318, Germany

10 \* Corresponding author: carsten.vogt@ufz.de

**KEYWORDS** H<sub>2</sub>, gas injection, subsurface, shallow aquifer, field scale, stable isotopes, hydrogenase

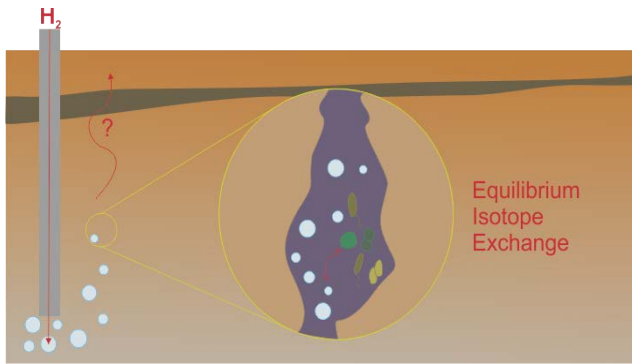
---

15 **ABSTRACT:** In the context of the shift towards clean, carbon-free energy, hydrogen (H<sub>2</sub>) receives growing attention as energy carrier. We monitored a simulated leakage of gaseous molecular H<sub>2</sub>, e.g. from a pipeline. H<sub>2</sub> was injected into a shallow aquifer and the resulting biogeochemical processes were monitored. For the first time, stable isotopes of hydrogen were used to track in situ H<sub>2</sub> transport and consumption. Isotopic composition of the injected H<sub>2</sub> was  $\delta^2\text{H} = -161.1 \pm 0.4 \text{ ‰}$ . During the injection, initial shifts in isotope signature of about  $\Delta^2\text{H} = + 8 \text{ ‰}$  in well D06 (1 m from injection) and of  $\Delta^2\text{H} = - 120 \text{ ‰}$  in well D04 (2 m from injection) were observed, probably caused

20 by a mass-dependent isotope effect associated with the pressure of the injection and the migration of the gas phase through pores and channels in the aquifer. After the injection, H<sub>2</sub>-concentrations decreased and an equilibrium isotope exchange with water lead to an isotopic depletion of H<sub>2</sub> ( $\delta^2\text{H} = -710.7 \pm 2.7 \text{ ‰}$ ) within 28 days, presumably catalyzed by hydrogenase enzymes of microbes. The theoretical equilibrium between H<sub>2</sub> and water was however not reached. We hypothesize that a continuous isotopic shift in the available H<sub>2</sub> due to physical transport processes resulted in a new isotope equilibrium with water, catalyzed by hydrogenases. Acetate detected in groundwater samples indicates *in situ* H<sub>2</sub>-oxidation by microbial homoacetogenesis. In laboratory experiments using H<sub>2</sub>-amended sediments sampled from the same site, microbial H<sub>2</sub>-oxidation was accompanied by equilibrium isotope exchange with water, and homoacetogenesis and ferric iron reduction were main microbial H<sub>2</sub>-consuming processes.

25 Overall, the H<sub>2</sub> isotope ratio was considerably impacted by physical and microbial processes occurring in the shallow aquifer. Monitoring of the equilibrium isotope exchange between H<sub>2</sub> and water could be used as a proxy for ongoing microbial H<sub>2</sub>-oxidation.

---



35

## INTRODUCTION

In the bid to transition towards renewable energy, hydrogen ( $H_2$ ) receives growing attention. In a future ‘hydrogen economy’,  $H_2$  could be used as a feedstock for chemical syntheses, as fuel or as an energy carrier. In addition, renewably-produced  $H_2$  has the potential to decarbonize key industries<sup>1,2</sup>. In order to become an intrinsic part of an energy system,  $H_2$ -ready storage and transport systems are needed.

However,  $H_2$  is a reactive gas with the potential to drive biogeochemical processes upon storage in geological sections such as salt cavern or exploited natural gas reservoirs and thereby lowering gas quantity by consumption, as well as quality with byproducts, e.g. hydrogen sulfide ( $H_2S$ )<sup>3,4</sup>. Moreover,  $H_2$  could potentially leak accidentally from geological  $H_2$  reservoirs or  $H_2$  pipelines into shallower formations and aquifers used as water resources due to the mobility of  $H_2$  gas and fast travel through geologic layers<sup>4</sup> and/or leaky wells<sup>5,6</sup>.

Finding, tracking and monitoring plumes and leakages are important aspects of the implementation of storage and transport systems. For this, isotope-based methods are often used, since they allow tracing gases in natural abundances *in situ*<sup>7-10</sup> and the isotopic signature of a compound is usually independent of its concentration. Similar field-scale experiments as described in this study for  $H_2$  injection have been performed with other gases. For example, successful monitoring of the distribution of injected  $CO_2$  or  $CH_4$  in shallow aquifers by  $\delta^{13}C$ -measurements was previously reported<sup>8-10</sup>.

In general, there are two different types of isotope effects: (i) *kinetic* isotope effects and (ii) *equilibrium* isotope effects<sup>11,12</sup>. Kinetic isotope effects can be used to track bond-change reactions, light isotopes usually react faster than heavy isotopes during bond-breakage. Thus, the remaining fraction of the compound becomes isotopically enriched over time.

Equilibrium isotope fractionation is understood as the partial separation of isotopes of one or more compounds being in chemical equilibrium, the isotopes are exchanged in an equilibration reaction<sup>11-13</sup>.  $H_2$  can exchange isotopes with water in an equilibrium reaction<sup>14-17</sup>. Without a catalyst, whether enzymatic or abiotic, this exchange is not measurable at room temperature within 18 days<sup>16</sup>.

Other important isotopic processes during a field-scale gas injection into the subsurface could be mass-dependent kinetic isotope effects<sup>11</sup>. There is a mass-dependent isotope effect in gasses, as their ratio of diffusion coefficients is equivalent to the inverse square root of their masses (Graham’s law)<sup>18-21</sup>. In laboratory experiments, migration affected the isotope signal of  $CH_4$ , as it shifted the carbon isotope signature from thermogenic towards the range of biological origin<sup>22,23</sup>. In the subsurface, isotope fractionation by migration of methane in a high temperature (90 °C), high-pressure regime (90 bar) has been measured<sup>24</sup>. In the field, sediment porosities, and thus effective migration pathways could further exacerbate this mass-dependent isotope effect. Field site injections have shown formation of channels and thus preferential pathways<sup>25</sup>, as well as differences in hydrogeology and content of solved ions in the groundwater<sup>25-27</sup>.

The goal of our study is to test and apply monitoring tools based on stable isotopes to assess the fate of subsurface  $H_2$ -plumes generated by leakage of  $H_2$  from e.g. geological storage or gas transport systems. We followed a  $H_2$  injection into the subsurface by monitoring its transport behavior and subsequent microbial degradation using compound specific stable isotope analysis (CSIA).  $H_2$ -oxidation by microbial communities of aquifer sediments from the field site were additionally investigated in laboratory microcosm experiments. This field-scale study is, to our best knowledge, the first in which gaseous  $H_2$  was directly injected into a shallow aquifer and

75

subsequent biogeochemical processes were monitored using CSIA. In order to catch reactive processes with high sensitivity, we tracked the gas injection by analyzing the isotopic composition of H<sub>2</sub> and CO<sub>2</sub>.

## MATERIALS AND METHODS

### Field site and equipment.

- 80 The field site *TestUM* is located in northern Germany (see Fig. 1), near the city of Wittstock/ Dosse in the federal state of Brandenburg (N 53° 11' 38.9616, E 12° 30' 11.178). The field site has been previously used for *in situ*-experiments to investigate the biogeochemical and hydrogeological effects of injected CO<sub>2</sub> or heat<sup>9,28,29</sup>. The area is composed of heterogeneous glacio-fluvial sediments from the Pleistocene, ranging from sands, clay and silts typical for sandurs to glacial loam and tills from the Saale and Vistula ice ages. Geological formations are tilting in western direction. Aquifers at this field site are found to be heterogeneous and comprised of fine to medium sand and delimited by discontinuous low permeability layers (aquitards), which vary in thickness and depth (see Figs. 1 and S1). High resolution vertical logs performed by a direct push hydraulic profiling tool (HPT; Geoprobe®, USA) confirmed different hydrostratigraphical units for the aquifers in the chosen injection site (see SI-1.1). The groundwater flows slowly west to southwestwards and drains into the river Dosse<sup>9</sup>, groundwater flow velocities were estimated to be about 0.3 m d<sup>-1</sup> in this area with strong local heterogeneities.
- 85
- 90

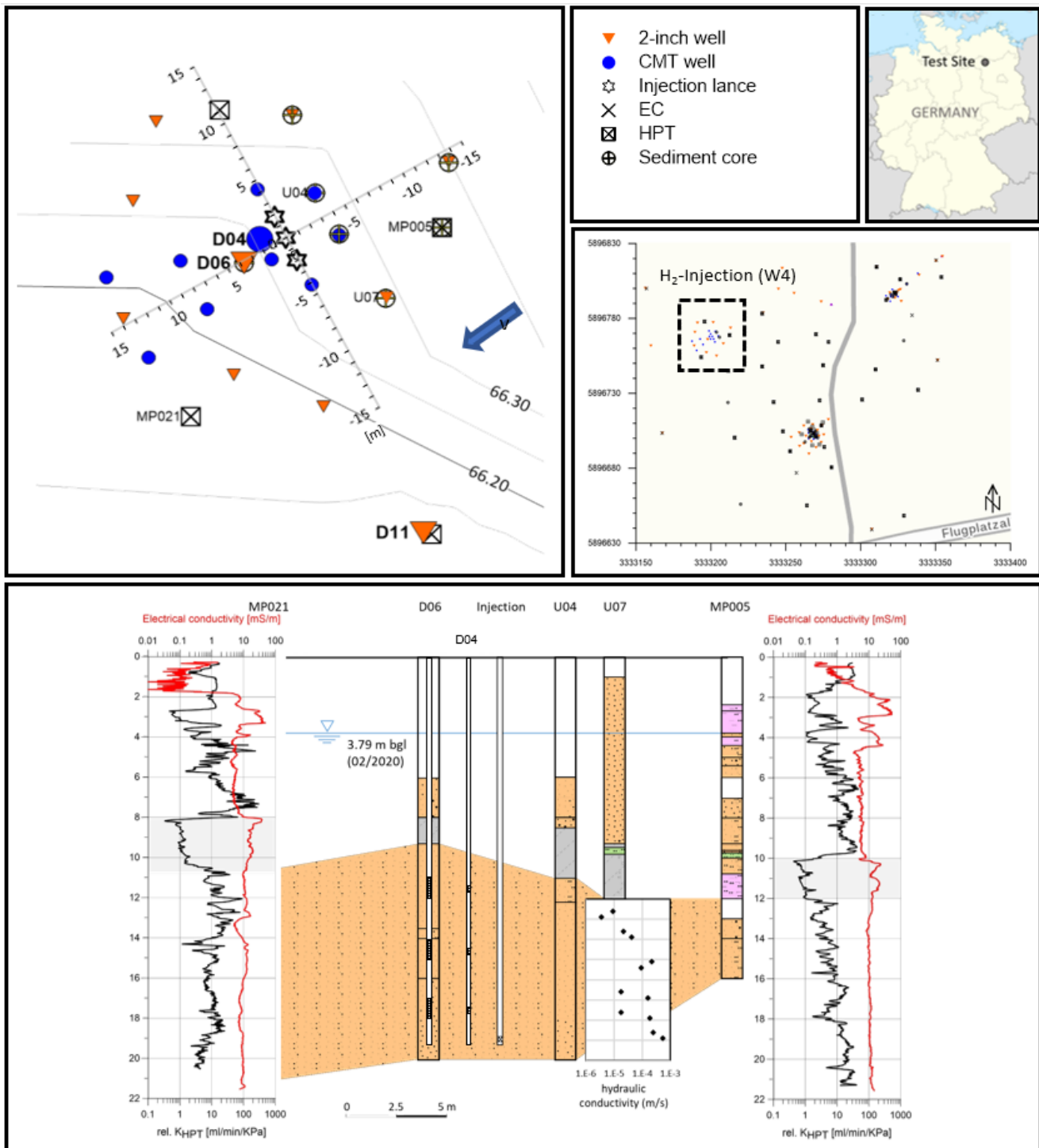


**Figure 1.** Field test site “TestUM” and its location in Germany (top right) and a detailed plan of the monitoring network for the H<sub>2</sub> injection test (top left) with water flow in south west direction (v), emphasized wells (D04, D06, D11) considered within this study, and a geologic profile (bottom) in flow-direction based on sediment (MP005, U07, U04, D06, MP021), as well as results of two HPT/EC-Logs (MP005, MP021) and examples for the positions of the filter screens at both types of groundwater wells (2-inch (D06) and CMT (D04)).

95

The isotope monitoring of the field experiment started in January 2020, with a baseline measurement in week 2 (2020/01/07 to 2020/01/08) and the H<sub>2</sub> injection in week 5 (2020/01/28 to 2020/01/30). Samples for isotope analyses were taken until week 16 (2020/04/15 to 2020/04/16).

Gas injection.

100

H<sub>2</sub> (N5.0; AirLiquide, France) was injected in a depth of about 18 m bgl (below ground level) through three continuous multichannel tubes (3-CMT; Solinst®, Canada) installed in a transversal distance of about 2 m (Fig. S1,

105 S2). In total, about 12 kg of H<sub>2</sub> were injected intermittently with seven injection phases (1h, 2h, 3h, and 4 x 6h) and six interruptions (1h, 2h, 3h, and 3 x 6h) (Fig. S3) over 54 hours through a 20 cm filter screen between 18.1 and 18.3 m bgl (below ground level) to generate a coherent gas phase and dissolved H<sub>2</sub>-plume. For the first three hours the flow rate was 13.4 mol min<sup>-1</sup> (300 NL min<sup>-1</sup>) H<sub>2</sub>. As some outgassing through monitoring wells near the injection wells was observed, the flow rate was then reduced to 1.8 mol min<sup>-1</sup> (40 NL min<sup>-1</sup>) H<sub>2</sub> for the next 27 hours to minimize H<sub>2</sub>-loss to the atmosphere and thus the uncertainty in the gas mass remaining in the aquifer. The reduced flow rate yielded slight overpressure (3 bar). Specific information on the provision of H<sub>2</sub> is described in the SI.

#### 110 Field sampling.

Three wells were selected for isotope monitoring (Fig. 1). Two of these (D04, D06) were close to the injection wells, where we expected to observe high H<sub>2</sub>-concentrations, and D11 served as control. Both D06 and D11 are 2"-wells (UTK-EcoSense GmbH, Germany), whereas D04 is a CMT-well (Solinst©, Canada) with three depths: 11.5 m, 14.5 m and 17.5 m. Wells were lined with high density polyethylene (HDPE). All samples were taken from 14.5 m (CMT-well) or from a filter screen from 14 to 15 m (2"-wells) bgl with the exception of D04 on day 2. Sampling in the injection period only took place during pauses of intermittent injections.

120 Groundwater was pumped up from CMT-wells with a peristaltic pump (24v DC 125 RPM; Verder Deutschland GmbH & Co. KG; Germany) and from 2"-wells with a submersible pump (Whale submersible electric galley pump; Munster Simms Engineering Ltd., Northern Ireland); it then flowed through an array of multiparameter probes (Profiline 1970i, WTW, Germany) to measure the on-site parameters pH, electrical conductivity, oxygen concentration and the redox potential. 60 to 100 ml groundwater were collected in borosilicate glass serum bottles and crimped closed with chlorobutyl-isoprene stoppers and aluminum caps for isotope analyses. The serum bottles had a volume of 120 ml, were pre-filled with approx. 5 g NaCl and autoclaved. The groundwater was sampled into the prepared bottles which were immediately closed after sampling. The addition of salt decreases the solubility of H<sub>2</sub>, supports partitioning into the head space in order to measure gaseous H<sub>2</sub>, and inhibits microbial activity.

125 For H<sub>2</sub>-concentration analyses, 20 mL GC-vials (prefilled with 1.8 g NaCl to inhibit microbial H<sub>2</sub>-conversion) were filled with 5 mL water and directly closed with crimp caps. The closed GC-vials were stored upside down in a refrigerator until analysis.

130 For sulfide determinations, 5 ml groundwater samples were filtered (0.2 µm) and stored cool in 8 ml disposable centrifuge tubes (Sarstedt AG & Co. KG, Germany) after stabilization with three drops 1 M NaOH.

#### Isotope Analyses.

135 The isotope ratios are shown in the δ-notation (see SI-4.1). The <sup>13</sup>C isotope ratio of CO<sub>2</sub> and potentially CH<sub>4</sub> in field and laboratory samples were measured with a gas chromatography-combustion-isotope ratio mass spectrometer (GC-C-IRMS) setup, which consists of a 6890A GC (Agilent Technologies, Germany) coupled to a MAT 253 IRMS (Thermo Fisher, Germany) via GC Combustion III (ThermoQuest Finnigan, Germany). The oxidation reactor was kept at 940 °C, the reduction reactor at 200 °C and the injector at 250 °C. Peaks were separated on a PoraBond Q column (Agilent Technologies, Germany) at 40 °C and 2 ml l<sup>-1</sup> He-flow. Limit of detection for δ<sup>13</sup>C-measurements is about 10 nmol C.

140 Hydrogen isotopes were measured on a different GC-IRMS setup, where a 7890A GC (Agilent Technologies, Germany) was coupled to a MAT 253 IRMS (Thermo Fisher, Germany) via Conflo II (Thermo Fisher, Germany). The injector was kept at 220 °C, the empty ceramic reactor tube was heated to 1420 °C and the helium-flow was adjusted to 1.2 min l<sup>-1</sup>. For the separation of permanent gasses, a Carboxen 1010 PLOT column (Supleco, Germany) was used. To allow potential measurements of CH<sub>4</sub> of the field samples, the temperature program was as follows: 40 °C for 3 min, ramp with 20 °C/min to 90 °C, hold for 6 min, ramp to 200 °C with 20 °C/min and hold for 2 min. The laboratory samples were measured isothermally (40 °C). Limit of detection for δ<sup>2</sup>H-measurements was about 100 nmol H. Precision of technical replicates was below ±1‰ for most measurements. Sampling the groundwater of the same depth twice and measuring these two samples led to isotopic values of -223.1 +/- 0.9 ‰ and -224.7 +/- 0.2 ‰, respectively, for D04 on day 2 at 11.5 m bgl (Fig. S5).

150 After isotope measurements of both δ<sup>13</sup>C-CO<sub>2</sub> and δ<sup>2</sup>H-H<sub>2</sub>, field site samples were acidified by addition of 6 N HCl and δ<sup>13</sup>C-CO<sub>2</sub> was measured again in order to assess the isotope signature of the complete inorganic carbon pool, independent of pH (see SI-1.4).

## Chemical Analyses.

155 H<sub>2</sub>-concentrations were analyzed on a GC-TCD (thermal conductivity detector) system. The GC-TCD system (7890B Agilent Technologies) for H<sub>2</sub>-analysis is connected via pro-steel transfer line with a headspace sampler (7697A Agilent Technologies). The injection system, working at 100°C, was equipped with a split/splitless injector and 1ml sample volume (out of headspace sampler loop) was injected with a split ratio of 1:5 into the GC system. The compound separation was realized by a Molsieve column (Agilent J&W/HP-Molsieve 30 m x 0.53 mm x 50.0 μm) as a pre-column and a Plot Q column (Agilent J&W/HP-Plot/Q 30 m x 0.53 mm x 40.0 μm) as the analytical column. Argon was used as carrier gas with a column flow of 36.3 ml min<sup>-1</sup>. The temperature oven program was running isothermally at 30°C. A TCD at 250°C was used for detection. Analytical uncertainty was 5 to 160 10%.

The GC-IRMS-analyses also allowed for an estimation of H<sub>2</sub>-concentration (see SI-1.5), which yielded lower values throughout.

165 Acetate and formate were determined by ion chromatography (IC; Metrohm-IC 881, Metrosep A Supp 5 - 150/4.0; Deutsche Metrohm GmbH & Co. KG, Germany), detection limits were <0.4 mg/l and <0.8 mg/l, respectively. Sulfide concentrations were determined photospectrometrically (Specord 50; Analytik Jena AG, Germany) with a Spectroquant® sulfide test (Merck, Germany). Aqueous oxygen concentrations in groundwater samples were analyzed electrochemically by an oxygen sensor (WTW CellOx 325 in a WTW Oxi 197 I device, Xylem Inc., 170 USA).

The concentration of dissolved inorganic carbon (HCO<sub>3</sub><sup>-</sup>) was determined with an alkalinity Gran titration; total inorganic carbon (TIC) and CO<sub>2</sub> (aq)-concentrations could be calculated with the hydrochemical modelling program Phreeqc (v3; phreeqc/Inl databases)<sup>18</sup> by using the groundwater composition as input parameters (data not shown).

175 Pure H<sub>2</sub> taken directly from the bottles in the field (2020/02/18, 25 bar left) was collected as a reference to obtain the <sup>2</sup>H isotope composition of the injected gas. The H<sub>2</sub> was flushed through an empty 120 ml-serum bottle and crimped closed with a chlorobutyl-isoprene stopper and an aluminum cap. Subsequently, 1 ml sample was then diluted in a 10 ml-vial prefilled with He for stable isotope measurement.

## Laboratory Microcosm Experiments.

180 Laboratory microcosm experiments were performed using sediment and groundwater from the field site, sampled in November 2019 from borehole U00 and MP005 in 11.5 m bgl to observe isotope fractionating processes under controlled conditions. A microcosm series was set up in 120 ml, autoclaved serum bottles and then continuously monitored in two independent, consecutive experiments with different H<sub>2</sub>-concentrations in the headspace. More information regarding microcosm set-up, experimental conditions, sampling procedures and analyses of chemical parameters is given in SI-2. 185

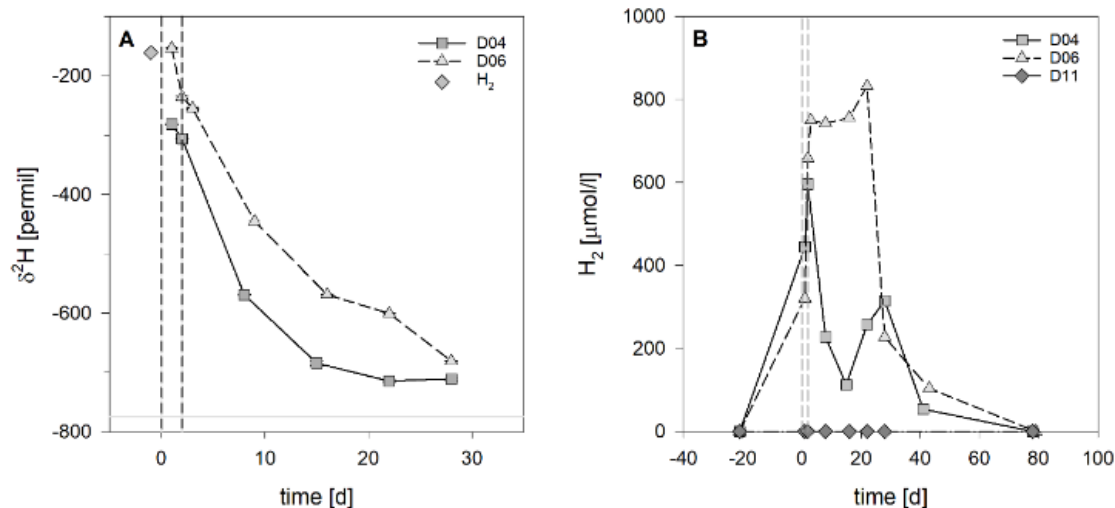
## RESULTS

### Field Site.

#### H<sub>2</sub>-Concentrations and Isotope Composition.

190 H<sub>2</sub> was injected into a shallow aquifer over the course of two days. It was not detected in any well prior to injection and not at all in the reference well D11 during the whole measurement campaign for isotopic samples. During the first three hours of injection close to the injection wells some outgassing of H<sub>2</sub> gas was observed in wells close to the injection (D07, D06, D04). This imply the formation of a rapidly ascending gas phase probably migrating upwards along major pores displacing ground water.

195 During the injection, higher H<sub>2</sub>-concentrations were observed in D04 compared to D06 (Fig. 2). Afterwards, D06 yielded higher concentrations throughout. We detected no H<sub>2</sub> in reference well D11. H<sub>2</sub> injected into the aquifer had a δ<sup>2</sup>H-value of -161.1 ± 0.4 ‰. D04 and D06 showed initial δ<sup>2</sup>H-values of -281.7 ± 0.7 ‰ and -152.5 ± 0.2 ‰, before becoming isotopically lighter, showing values of -710.7 ± 2.7 ‰ and -680.9 ± 0.9 ‰ at day 28 (see Fig. 2A).



200 **Figure 2.**  $\delta^2\text{H}$  values (A) and concentrations (B) of  $\text{H}_2$  in the water phase of field samples from D06 and D04 (14.5 m depth);  $\text{H}_2$ -concentrations for reference well D11 are also shown (B). The isotope signature of the injected  $\text{H}_2$  is shown in (A) for comparison. Vertical lines delimit the injection period and isotope samples are shown as mean with standard deviation.  $\text{H}_2$  was not detected in samples from the reference well D11. Hydrogen isotopes of  $\text{H}_2$  tend towards equilibrium with water ( $\delta^2\text{H} = -775 \text{‰}$ , shown in light grey), but stabilize around  $\delta^2\text{H} = -710 \text{‰}$  in D04.  $\text{H}_2$ -concentrations spike shortly in D04 after the injection period before decreasing. In contrast, D06 yields high concentrations until day 28. Due to the intermittent sampling schedule, no samples are available for D04 on day 3.

205

During injection at day 2, isotopes of  $\text{H}_2$  were measured in three depths of D04 (Fig. S5 A). The  $\delta^2\text{H}$ -values differed, with 11.5 m bgl yielding the isotopically heaviest ( $\delta^2\text{H} = -223.1 \pm 0.9 \text{‰}$ ) and 17.5 m bgl the isotopically lightest values ( $\delta^2\text{H} = -431.3 \pm 5.0 \text{‰}$ ; Fig. S3A). Generally,  $\text{H}_2$ -concentrations in D04 were highest in 17.5 m and 14.5 m, and lowest in 11.5 m in the time course of the field experiment; in contrast,  $\text{H}_2$ -concentrations were considerably higher in 14.5 m and 11.5 m compared to 17.5 m in D06 (Fig. S6A-C).

210

#### Concentrations and Isotope Composition of $\text{HCO}_3^-$ and gaseous $\text{CO}_2$

$\text{HCO}_3^-$  and  $\text{CO}_2$  were monitored in the field in addition to  $\text{H}_2$ .  $\text{HCO}_3^-$ -concentrations remained fairly stable at 2  $\text{mmol l}^{-1}$  in D04 during the field experiment. In D06 and D11,  $\text{HCO}_3^-$ -concentrations decreased with injection (Fig. 3). On day 78, both D04 and D06 yielded elevated concentrations. Gaseous  $\text{CO}_2$  showed a slight increase in concentration in D11 after injection (Table S1).

215

Measurements of carbon isotopes of TIC (acidified samples, Fig. 3A) and gaseous  $\text{CO}_2$  (non-acidified, Fig. S7) samples showed a similar trend for both wells near the injection site. In general, the difference between the two wells was always about 2 ‰, with samples from D04 being isotopically heavier than those from D06. Initial  $\delta^{13}\text{C}$ -values were  $-11.9.0 \pm 0.1 \text{‰}$ ,  $-15.2. \pm 0.04 \text{‰}$ , and  $-16.8 \pm 0.2 \text{‰}$  for D04, D06, and D11, respectively. The reference well D11 differs (Fig. 3 B), as there was a drop to  $-17.2 \pm 0.1 \text{‰}$  on day 2. The depth profile of D04, taken on day 2, showed that TIC was slightly enriched in  $\delta^{13}\text{C}$  at 14.5 m depth (Fig. S5B).

220

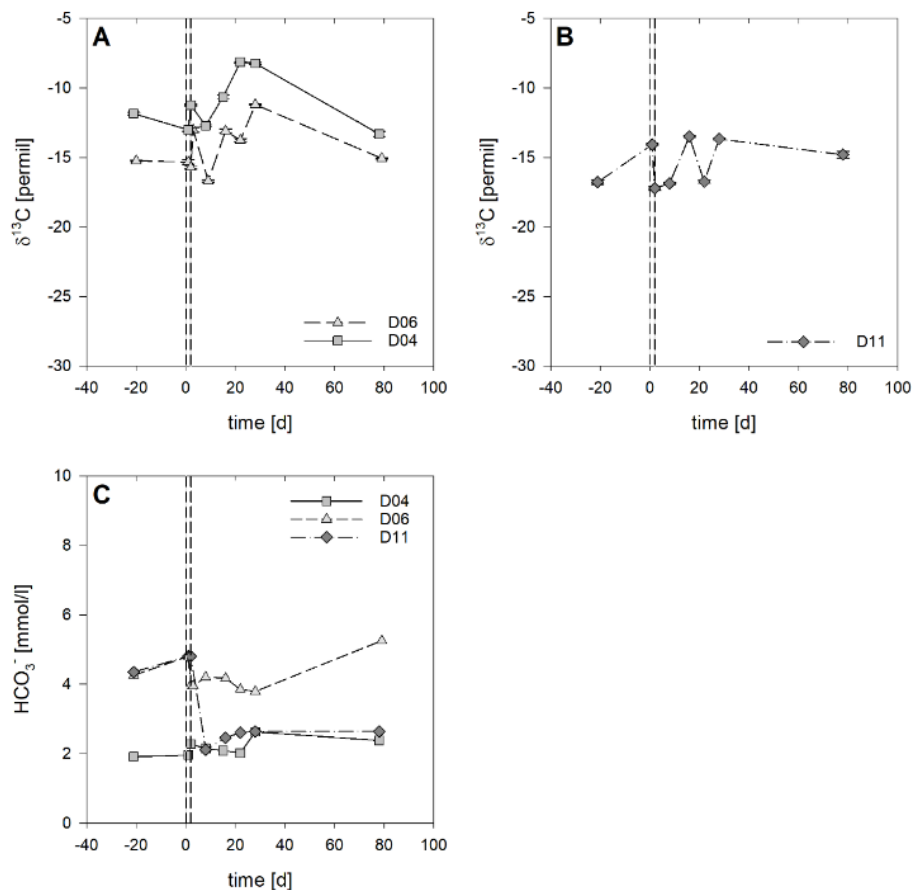


**Figure 3.** Carbon isotopes analyses of  $\text{HCO}_3^-$  in the sampling wells D06 and D04 (A) and the reference well D11 (B), after acidification of samples. Concentrations of  $\text{HCO}_3^-$  are shown in C. Vertical lines delimit the injection period and isotope samples are presented as mean with standard deviation of technical replicates.

#### Geochemical Parameters.

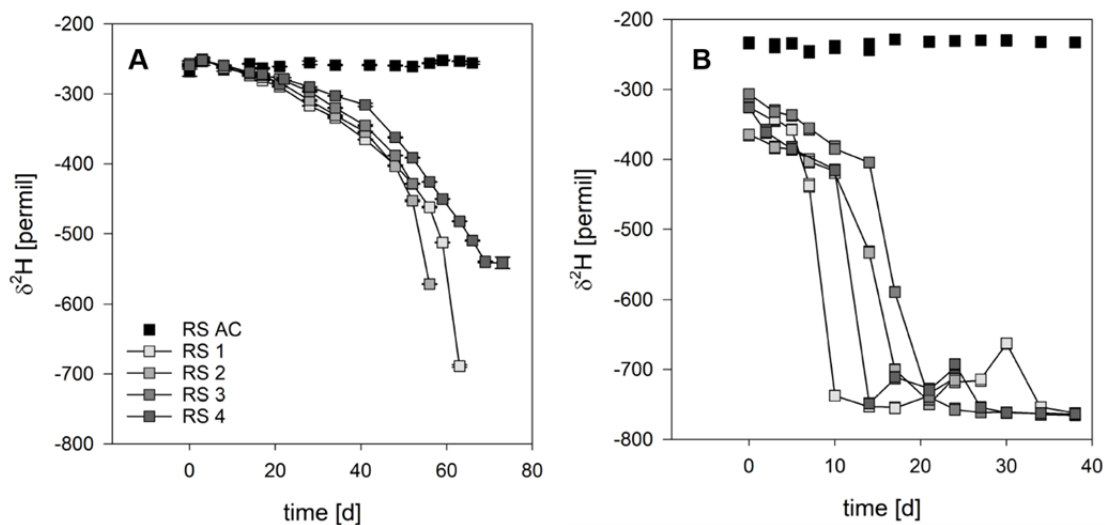
The geochemistry of the test site was comprehensively monitored to allow subsequent tracking of geochemical changes due to the injection of  $\text{H}_2$ . No sulfides could be detected in the reference well D11. In the other wells, sulfides were sporadically detected ranging from 3.6 to 42.3  $\mu\text{mol l}^{-1}$  (Tab. S2). Measured oxygen average concentrations after injection were below 65  $\mu\text{M}$  in D04 and D06, and 175  $\mu\text{M}$  in the reference well D11. The pH was fairly stable in well D06 during the experimental period, ranging from 7.2 to 7.6 (Fig. S4). In D04, the pH ranged from 7.8 to 8.0 from injection to day 28, slightly different to pre-injection (7.3). At day 78, pH had decreased to 6.8. D11 showed an increase from 6.9 to 7.3 during the injection period, before decreasing to 6.5  $\pm$  0.2 for all measurements from days 2 to 78. This pH value remained below the pre-injection value.

In both D04 and D06, acetate was detected after the injection; but not in D11. Before and during the injection, acetate concentrations were below limits of detection. Acetate concentrations in D04 ranged from 61.0 to 71.1  $\mu\text{mol l}^{-1}$  without significant de- or increase at  $t = 14$  d,  $t = 21$  d and  $t = 28$  d. It was not detected at day 78. In D06, acetate concentrations increased from 27.1  $\mu\text{mol l}^{-1}$  at day 21 to 159.2  $\mu\text{mol l}^{-1}$  at day 28, before decreasing to 22.0  $\mu\text{mol l}^{-1}$  at day 78. In D04, 28.8 and 35.6  $\mu\text{mol l}^{-1}$  formate were detected at days 21 and 28, respectively. At day 28, 60.9  $\mu\text{mol l}^{-1}$  formate were measured in D06. In the reference well D11, acetate was always below the detection limit.

#### Laboratory Microcosm Experiments.

Two consecutive experiments were performed with sediment and groundwater from the field site. In the first experiment, conditions after injection in the central plume were simulated by adding high concentrations of  $\text{H}_2$ . In the second experiment, conditions at the edges of the plume, months after injection, were simulated by adding lower concentrations of  $\text{H}_2$ .

250  $H_2$  was consumed and became isotopically lighter compared to the abiotic control ( $\delta^2H = -780 \text{ ‰}$ ), due to the superimposing equilibrium exchange reaction with water as previously observed<sup>16</sup> (Fig. S8, S9). Hydrogen oxidation in the first experiment could not be clearly quantified by GC-IRMS concentration analyses, indicating substantial losses of  $H_2$  before measurement. This emphasizes the sensitivity of the isotope analysis, which indicated microbial activity after an initial lag phase of 17 days (Fig. 4). In the second experiment with limited  $H_2$ -content, the  $H_2$ -isotope exchange was completed within around 20 days (Fig. 4).



255 **Figure 4.** Hydrogen isotopes analyses of  $H_2$  over time in the first (A) and the second experiment (B). RS 1-4 are biotic replicate microcosms, RS AC is an abiotic control microcosm.

260 There was little shift in the  $\delta^{13}C$ - $CO_2$  composition in the first experiment. After 52 d,  $\delta^{13}C$ -values for  $CO_2$  of up to +4 ‰ for half of the replicates were observed (Fig. S10), whereas the abiotic control remained stable over time. Notably, the consecutive setup leads to isotopically enriched  $CO_2$  at the start of the second experiment. Subsequently,  $\delta^{13}C$ - $CO_2$ -values above +40 ‰ were detected for some replicates (Fig. S11), indicating strong isotope fractionation upon  $CO_2$ -consumption. Fe(II)-concentrations increased starting from day 48 in the first experiment, yielding values above 1 mM for all replicates (Fig. S12). Acetate concentrations increased up to 17.0 mM in all biotic microcosms at the end of both experiments, whereas formate was detected (27.2  $\mu M$  maximum) in three out of four microcosms (Tab. S4).

## DISCUSSION

270 Gaseous  $H_2$  was injected into a shallow aquifer and subsequent reactive processes of  $H_2$  and  $CO_2$  were monitored with stable isotopes for the first time. In previous studies, the equilibrium isotope exchange of  $H_2$  with  $H_2O$  was shown to be associated with enzymatically-catalyzed  $H_2$ -oxidation<sup>30-32</sup> and its characteristic shift towards isotopically lighter  $H_2$  could be tracked in laboratory experiments using a model  $H_2$ -oxidizing microbial strain<sup>16</sup>. Hence, we hypothesized that we could use this principle for qualitative monitoring of microbial  $H_2$ -oxidation at a field scale.

275 Similar field-scale gas injection experiment has been performed with  $CO_2$  at our field site<sup>9</sup>, whereas a  $CH_4$  injection field experiment has been recently carried out in a Canadian aquifer<sup>10</sup>. The distribution of injected  $CO_2$  or  $CH_4$  in these shallow aquifers was monitored by  $\delta^{13}C$ -measurements<sup>9,10</sup>. The migration of the  $CO_2$  plume at our field site was reported to be slow<sup>9,33</sup>. In comparison to  $CO_2$ - or  $CH_4$ -injections, the detection of  $H_2$  with hydrogen stable isotopes in the sampling wells was only possible over a short time period, demonstrating the high reactivity and fast dispersion of  $H_2$  in the aquifer.  $H_2$  could only be detected in the selected wells until day 28 with CSIA, whereas  $\delta^{13}C$ -monitoring for  $CO_2$  and  $CH_4$  in similar field experiments was possible over more than 200 days<sup>9,10,33</sup>. At our site, the glacio-fluvial sediments with different hydrostratigraphical units, lenses and cross stratification form a heterogenic subsurface geology with changing permeability and redox conditions promoting micro-oxic to anoxic niches. In this field experiment, conditions in the aquifer were micro-oxic to anoxic, confirming previous oxygen measurements in the course of a  $CO_2$  injection experiment<sup>9</sup>.

285 As the groundwater flow was relatively slow with about  $0.3 \text{ m d}^{-1}$  and strong heterogeneities due to the varying  
glacial sediments, we assume that the flow is no decisive factor for the fast dispersal of  $\text{H}_2$  in the subsurface. The  
gas injection itself will thus initially influence the dispersion of  $\text{H}_2$  within the aquifer. It is known from former gas  
injection field experiments that the injected fugitive gas migrates as free phase in different directions and dis-  
solves gradually in groundwater during transport<sup>34</sup>. It has been shown that a gas injection into water-filled sedi-  
290 ment forms channels through which the gas phase will then migrate preferentially upwards in form of bubbles<sup>35-  
37</sup>. When the injection and subsequently, supply of gas is halted, these channels collapse, as observed in a  $\text{CH}_4$ -  
injection experiment<sup>10</sup>. At the field site,  $\text{H}_2$  was injected with over pressure at about 18 m bgl to generate a co-  
herent gas phase and dissolved  $\text{H}_2$ -plume (cf. SI-1). The observed outgassing of  $\text{H}_2$  through monitoring wells dur-  
ing the injection of  $\text{H}_2$  implies a buoyancy-driven upwards migrating  $\text{H}_2$  gas phase. The actual geometry of such  
295 channel systems depend on various aspects, such as imbedded silty layers, but has been shown to be parabolic,  
and the density of channels and gas should be highest directly below and close to the injection point<sup>35-38</sup>. In  
D06, which is more distant to the injection site compared to D04, the  $\text{H}_2$ -concentration in 11.5 m and 14.5 m bgl  
were higher than in 17.5 m bgl after the injection (Fig. S4). This indicates anisotropic dispersion and a pro-  
nounced migration along channels upwards with increasing distance. The higher  $\text{H}_2$ -concentrations closer to  
300 ground level after the injection period indicate that this gas transport continues after injection and that the rise  
of  $\text{H}_2$  is hindered by layers with low permeability, i.e. silt, clay and loam, as described previously<sup>4</sup>. This observa-  
tion suggests a preferential migration of gas along channels as previously observed<sup>25</sup>. There were no indications  
that  $\text{H}_2$  spread over a large area in other wells at the site.

The injection of gas should lead to displacement of an equal volume of water<sup>38</sup>. As the sediment of the aquifer  
is not homogeneous, the geology not uniform, and the gas distribution unequal along the depth profile, simple  
305 isotropic displacement of the water is unlikely. There are indications that this water was, at least partly, dis-  
placed in a south-western direction, indicated by a shift in pH and concentrations of carbonate in D06 and D11;  
influx of displaced water with dissolved  $\text{HCO}_3^-$ , would lead to new equilibration of  $\text{HCO}_3^-$  with matrix carbonates  
and may be accompanied with a change of pH<sup>39</sup>. We observed that the  $\text{CO}_2$ -concentration in D11 increased with  
the injection while the pH slightly rose from 6.9 (day -21) to 7.3 (day 1), before concentration sharply decreased  
310 (Fig. 3), and the pH stabilized at about 6.4 without detection of  $\text{H}_2$  (see Fig. S4). Overall, we therefore assume a  
preferential flow of displaced water in south-western direction.

We observed strong isotope effects of  $\text{H}_2$  over the course of the field experiment. Overall, our method is well  
suited for field investigations, as it assesses the isotope signal, which is independent of concentrations, and can  
determine the concentration at the same time. Thus, isotope analysis is an effective and reliable tool in this con-  
315 text. However, the composition of the hydrogen isotope signal can be influenced by both physical and biological  
processes. As there already was isotope fractionation observed during the injection itself, initial physical pro-  
cesses are more likely than rapid biological activity, due to common lag phases of microorganisms when con-  
fronted with new electron acceptors and donors<sup>40-42</sup>. A lag phase of 17 d days prior to  $\text{H}_2$ -oxidation was also ob-  
served in the laboratory experiment (Fig. S8). In addition, an increase in  $\text{H}_2$ -concentrations was observed during  
320 this time, whereas consumption of  $\text{H}_2$  - or no change in concentration in a steady-state system of consumption  
and supply - would be expected for a biotic process.

Physical processes that could affect the stable isotope signatures are complex interactions of mixing and dilution  
of  $\text{H}_2$  by inflowing water, directed flow, gas-water phase transitions and mass-dependent diffusive transport in  
the gas or liquid phase (see Fig. 4; cf. SI-3). Large stable isotope fractionation effects of  $\text{H}_2$  can be expected due  
325 to the large mass difference between hydrogen isotopes (1 u), affecting all transport processes to an extent<sup>11, 30</sup>.  
Transport processes would be further affected by sediment properties, pore volumes and tortuosity (cf. SI-3, SI-  
4.1 and SI-4.2)<sup>31</sup>.

Dilution and dispersion of  $\text{H}_2$  after injection into the saturated zone is largely dependent on groundwater flow  
rates and solubility of the compound. As discussed above, the groundwater flow was relatively low and the  $\text{H}_2$ -  
330 plume did not spread to all monitoring wells on site. Notably,  $\text{H}_2$  is barely soluble in water with a Henry's law  
solubility constant ranging from  $7.7$  to  $7.9 \times 10^{-6}$ <sup>43</sup>. Thus, with little evidence of fast lateral  $\text{H}_2$ -migration along  
groundwater flow and generally low solubility, we suggest that dilution and dispersion effects did not considera-  
bly influence the measured isotope signatures.

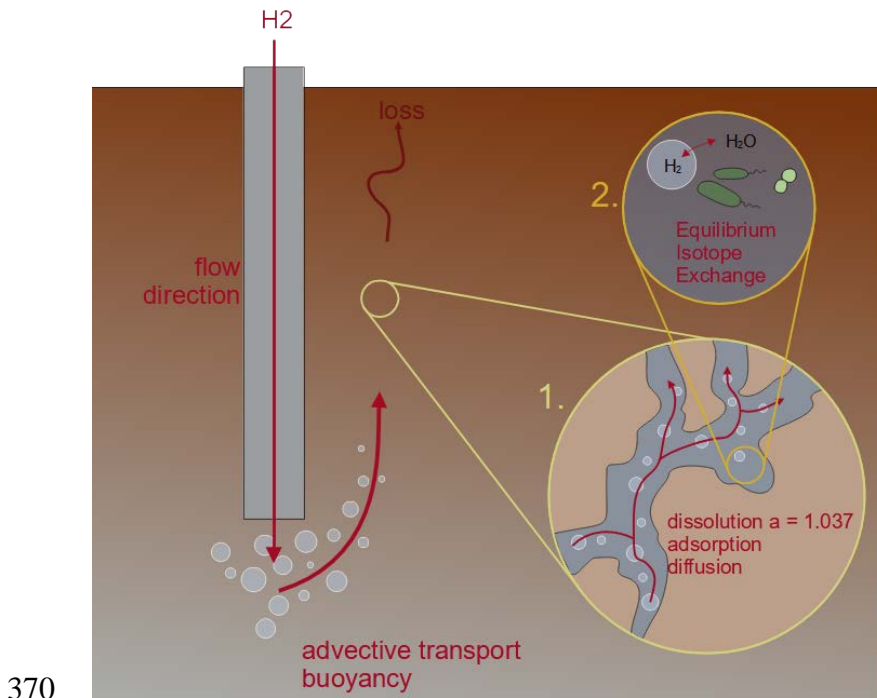
335 Injections of oxygen ( $\text{O}_2$ ) into subsurface aquifers resulted in a changing local water chemistry and a trapped gas  
phase of nitrogen ( $\text{N}_2$ ) due to replacement of dissolved  $\text{N}_2$  by dissolving  $\text{O}_2$ <sup>44,45</sup>. Analogously, injected  $\text{H}_2$  likely

displace dissolved N<sub>2</sub> so that a residual gas phase of H<sub>2</sub> and N<sub>2</sub> is formed. In addition, in high pressure regimes gas can affect the (dis-)solution of various compounds present in the water phase and could potentially affect mineral phases at the site<sup>46</sup>. Due to the low solubility of H<sub>2</sub> in water<sup>43</sup>, we presume that the initial gas bubbles in the subsurface may extract gases such as N<sub>2</sub>, by interphase transfer continuously enriching permanent gases in the gaseous phase which may affect further dissolution of H<sub>2</sub> in water<sup>46</sup>. Dissolution of gaseous H<sub>2</sub> in H<sub>2</sub>O is associated with an equilibrium isotope effect of  $\alpha = 1.007$  to  $1.037$ <sup>19,47,48</sup> due to the larger solubility of D<sub>2</sub> or HD<sup>49</sup>, which would favor an isotopic depletion of the gas phase. This would result in an isotope effect of about  $\delta^2\text{H} = 3$  ‰ according to Knox, Quay & Wilbur<sup>48</sup> using the initial  $\delta^2\text{H}$ -value of the injected H<sub>2</sub>. This 3 ‰-difference would not sufficiently explain the observed much larger isotope effects. But potentially, multiple phase transitions during the bubble transport of H<sub>2</sub> and continuous dissolution of the gas phase could add up to larger isotope effects. Here, along an open, wide channel, a larger gas phase will move over longer distances and becomes less enriched in light isotopes compared to a smaller gas phase moving through small channels.

In addition to this hydrogen isotope enrichment effect of continuous dissolution of the H<sub>2</sub> gas phase, we suggest an initial mass-dependent isotope effect, triggered by the initial high-pressure injection, affecting the isotope signal, as suggested in literature<sup>50,51</sup>. Modelling has shown that the pressure build-up during injection can be considerable in deep aquifers<sup>27</sup>. This could explain the sudden isotopic shift from the injection site to D04 one day after the injection, as well as the decreased rate of isotopic change from  $-120$  ‰ d<sup>-1</sup> to  $-25$  ‰ d<sup>-1</sup> in D04 and the different isotope values in different depths during the injection (see SI, Fig. S6).

Other isotope effects might be due to molecular diffusion as described for experiments with CH<sub>4</sub> which have shown a general depletion of diffused CH<sub>4</sub> compared to the source<sup>22,23</sup>. However, molecular diffusion of CH<sub>4</sub> through water saturated pores is a slow process<sup>22</sup>. Thus, diffusion alone is probably not a significant factor for H<sub>2</sub>-transport over longer distances in the relatively short time period of the experiment. Similarly, heavier species may adsorb on mineral surfaces or on disseminated organic matter as observed for CH<sub>4</sub><sup>22</sup>. Isotope segregation due to adsorption during migration of gas phases might contribute to isotope fractionation of H<sub>2</sub> in the early phase of the experiment. Segregation during migration is a diffusion-controlled process describing the interaction with aquifer matrix and dissolution of gas bubble moving through the saturated aquifer<sup>22</sup>.

In summary, we observed different H<sub>2</sub> isotope values in different depths in D04 during the injection itself (Fig. S6); this H<sub>2</sub> isotope fractionation is unlikely to be caused by biotically-induced equilibrium isotope effects due to its rapidity. Loss of H<sub>2</sub> due to outgassing to the surface was observed and suggest advective transport of gas bubbles. Our results show that there is no equal, uniform distribution of H<sub>2</sub> and the subsequent isotope signal, which suggests differences in sediments (e.g. grain size and distribution and its pore volumes), tortuosity and morphology (e.g. cross stratification) affect the distribution and isotope signal of H<sub>2</sub> in the subsurface (Fig. 5, cf. SI-4). Further studies under more controlled conditions are needed for a better understanding of the phenomenon.



370

**Figure 5.** Schematic overview over (1) physical processes affecting the H<sub>2</sub> isotope signal and (2) subsequent equilibrium isotope exchange between H<sub>2</sub> and water facilitated by microorganisms during injection.

The change in flow under a changed pressure regime caused by the injection might influence initial changes in the isotope signal, but it would not explain the isotope exchange even after the pressure dissipated. Besides  
 375 physical processes, biological activity can also affect the isotope composition. H<sub>2</sub>-oxidation catalyzed by the enzyme hydrogenase has been demonstrated to result in an equilibrium isotope exchange with water, leading to an isotopic depletion of H<sub>2</sub> <sup>14,52</sup>. This equilibrium isotope exchange superimposes kinetic isotope effects <sup>16</sup> and we therefore hypothesized that biological consumption of H<sub>2</sub> will lead to isotopically depleted  $\delta^2\text{H}$ -values of the gas phase in the field site. In order to observe this equilibrium isotope exchange, a catalyst is needed. There is no  
 380 difference in the equilibrium isotope fractionation for abiotic or biotic catalysts <sup>14,52,53</sup>. As the sediments at the field site do not contain abiotic catalysts in relevant concentrations, such as i.e. Pt, Pd, Ni, Rh or Fe(0), we assume no detectable abiotic equilibrium reactions took place during the first 28 days after injection. Laboratory tests showed no abiotic isotopic equilibration between H<sub>2</sub> and autoclaved groundwater with autoclaved sediment from the field site in 66 d (see SI-2.2). Also, since both well types were lined with HDPE, we assume no catalytic properties of the wells itself. Considering that the microbial community is adapted to the *in-situ* conditions and has not been exposed to different and unfavorable conditions, as sampling sediments for laboratory experiments tend to do, lag phases in reaction to the sudden H<sub>2</sub>-influx could be similar or even lower to the ones observed in the laboratory. In addition, H<sub>2</sub> is a universally used energy carrier across various microbial species, which carry a wide array of different hydrogenases <sup>54</sup>.

390 During our observation period, the  $\delta^2\text{H}$ -signal in D04 does not reach the equilibrium value of  $\delta^2\text{H} = -775$  ‰, calculated after Horibe & Craig <sup>55</sup> for  $T = 12$  °C with the isotopic composition of the field site's groundwater ( $\delta^2\text{H} = -61.9 \pm 3.3$  ‰, cf. SI-4.1). This offset between theoretical equilibrium and measured  $\delta^2\text{H}$ -values of about  $\Delta^2\text{H} = 65$  ‰ does not seem to be due to the sampling itself, as the H<sub>2</sub> that was injected only marginally differs from the initial  $\delta^2\text{H}$ -value in D06. Within the variability and measurement errors of the temperature and the isotope ratio of H<sub>2</sub>O of the field site, theoretical  $\delta^2\text{H}$ -values differ by approximately  $\pm 8$  ‰. A potential explanation for this offset might be found in the combination of counteracting isotope effects. Physical isotope effects would generally lead to an isotopic gradient with heavier isotopes near the source and lighter isotopes further away.

400 Activities of the enzyme hydrogenase would lead to an isotopic depletion of dissolved H<sub>2</sub> in the environment of the microorganisms<sup>14-16,31</sup>. During and shortly after the injection, sampling wells would first show isotopically light  $\delta^2\text{H}$ -values due to the combined effects of physical transport. Further migration would bring in isotopically heavier H<sub>2</sub> in the aqueous phase. If this isotopically heavier H<sub>2</sub> in the aqueous phase was used by microorganisms, the equilibrium values would shift accordingly. In order to reach an equilibrium shifted by  $\Delta^2\text{H} = 65$  ‰, the

starting value of the H<sub>2</sub> isotope signature should have been δ<sup>2</sup>H = +210 ‰. Due to continuous measurement of isotopically lighter values, we hypothesize that these processes were continuously taking place. We therefore suggest that an equilibrium isotope exchange measured over longer periods of time (approx. 15 d, see Fig. 2) at the same sampling point was largely influenced by hydrogenase activity and thus microbial H<sub>2</sub>-oxidation. Such analyses might be best suited for monitoring microbial activity and therefore gas quality within closed reservoirs.

There are various potential electron acceptors available for microbial H<sub>2</sub>-oxidation in the subsurface. In oxic environments, knallgas bacteria would consume H<sub>2</sub> and O<sub>2</sub> and form water<sup>56</sup>. In anoxic environments, different electron acceptors, such as nitrate, sulfate, Mn(IV) or Fe(III) could be used for H<sub>2</sub>-oxidation<sup>56–59</sup>. H<sub>2</sub>-oxidizers<sup>56</sup>, e.g. homoacetogens and hydrogenotrophic methanogens fix CO<sub>2</sub> chemoautotrophically and thus may additionally influence the CO<sub>2</sub>-equilibria and the pH. We observed production of formate and acetate, as well as indications for sulfate reduction in the field and the potential for iron reduction in laboratory experiments (see SI-1 and 2.2). Groundwater that is pumped to the surface always represents a mixture of groundwater in the subsurface, even if filter screens divide sampling ports. Therefore, local heterogeneities and ecological niches might not be represented in full.

Fe(III)-reduction started before changes in the δ<sup>13</sup>C-values of CO<sub>2</sub> became apparent in the laboratory experiments. Iron cycling can be a cryptic process, which could be coupled to sulfur (re-)cycling, even in low sulfate environments<sup>60</sup>. As there are indications for sulfate reduction at the field site (Tab. S1), such a cycle might be a possibility in parts of the subsurface.

We have not observed methanogenesis during the first 79 days after injection in the field or in the laboratory experiments. Instead, about 65 μM formate was measured in both D04 and D06 and, with the exception of one replicate, all laboratory microcosms contained formate, which can be formed directly from CO<sub>2</sub> and H<sub>2</sub> by the formate dehydrogenase. It can be an indicator for syntrophy, as it is often transferred between microorganisms<sup>61,62</sup>. Formate is also an intermediate during chemolithotrophic growth, which can accumulate transiently during H<sub>2</sub>-oxidation<sup>63</sup>.

In the field, homoacetogenesis was indicated with acetate production in D06 and D04 from days 21 on and in all active microcosms of the laboratory experiment (Tab. S2). High carbon isotope fractionation, as observed in the laboratory experiments (Δ<sup>13</sup>C ≥ +40 ‰), is associated with homoacetogenesis<sup>64</sup>. During homoacetogenesis, acetic acid is formed by reduction of two molecules of CO<sub>2</sub> by four molecules of H<sub>2</sub>. The formed acetate can be used by other microorganisms, such as methanogens and sulfate reducers<sup>64</sup>. Overall, the results suggest that homoacetogenesis is a dominant H<sub>2</sub>-oxidising process at this field site.

## CONCLUSION

Our findings implicate that monitoring of H<sub>2</sub> by CSIA can obtain information on both physical and biological processes. We could observe initial physical isotope fractionation during gas migration, followed by an isotope exchange reaction of H<sub>2</sub> with water catalyzed by the enzyme hydrogenases. The isotope fractionation associated with migration likely led to an isotopically heavier H<sub>2</sub>, which was used by microorganisms. The interaction of these processes resulted in a new isotope equilibrium, shifted by about Δ<sup>2</sup>H = 65 ‰.

The microbial community at this field site is able to oxidize H<sub>2</sub> by Fe(III) reduction, homoacetogenesis and potentially sulfate reduction. Further studies and continued observation of long-term effects, such as changes in the microbial community, acidification or production of methane from acetate, are important to assess the impact of potential leakages of H<sub>2</sub> from pipelines on the microbial community, the sediment and the water quality.

Isotope analysis of microbial H<sub>2</sub>-consumption in the subsurface *in situ* is generally possible and the observed equilibrium isotope exchange of H<sub>2</sub> with water can serve as proxy for biological activity and thus for consumption in storage systems. Physical processes associated with gas migration, especially during injection, can camouflage the biological isotope exchange reaction with water and may lead to a new equilibrium. Hydrogen isotope analyses are generally well suited for monitoring of H<sub>2</sub> in closed reservoirs or storage solutions, as they are not dependent on concentrations and can give rapid insights into biological activity.

## 450 ASSOCIATED CONTENT

Supporting Information.

SI-1: Additional Field Data

SI-2: Laboratory Microcosm Experiment  
SI-3: Gas Distribution during Injection  
455 SI-4: Calculations & Equations

## AUTHOR INFORMATION

### Corresponding Author.

\* Carsten Vogt

460 Department Isotope Biogeochemistry, Helmholtz Centre for Environmental Research – UFZ, Permoserstr. 15,  
Leipzig 04318, Germany. E-mail: carsten.vogt@ufz.de

### Author Contributions.

465 ML prepared the manuscript, collected and analyzed the isotopic field data and designed the laboratory experi-  
ment. MS executed the laboratory experiments. CV and HHR conceptualized the project, supported the interpre-  
tation of the data and reviewed the manuscript. AD commented on the manuscript. GH and KL coordinated the  
field experiment, reviewed the manuscript and completed parts of the methods section. UW coordinated the  
geophysical field investigations and provided additional information, graphs and text on direct push-based meth-  
ods.

### Funding Sources.

470 This work was supported by the Federal Ministry for Economic Affairs and Energy (BMWi) within the funding ini-  
tiative “Energiespeicher,” project ANGUS II, Grant Number 03ET6122B, and by the Bundesministerium für Bild-  
ung und Forschung (BMBF) within the funding initiative “Forschung für Nachhaltige Entwicklung (FONA3)”, pro-  
ject TestUM-Aquifer (grant number 03G0875B).

## ACKNOWLEDGMENT

475 We are grateful for the help of Nilufar Zarrabi and Nina Sophie Keller during field sampling. We would like to  
thank Steffen Kümmel for help in the isotope lab. We are also very grateful for Helmut Geistlinger’s explanations  
of the geometry of gas injections. We acknowledge Maike Schulz, who measured the isotopic composition of the  
field site’s groundwater during an internship in 2018. IC measurements were conducted by the analytical service  
of the Helmholtz Centre for Environmental Research by Maria Ullrich and Michaela Wunderlich. In addition, we  
would like to acknowledge Marco Pohle, who helped in the assembly of figure S1. Slug tests at the field site were  
480 performed by Susann Birnstengel.

## References

- (1) European Commission. *A hydrogen strategy for a climate-neutral Europe*.
- (2) Bundesministerium für Wirtschaft und Energie. *Die Nationale Wasserstoffstrategie*.
- (3) Gregory, S. P.; Barnett, M. J.; Field, L. P.; Milodowski, A. E. Subsurface Microbial Hydrogen Cycling: Natural  
485 Occurrence and Implications for Industry **2019**, *Microorganisms* (7 (2)), 27.
- (4) Hagemann, B.; Rasoulzadeh, M.; Panfilov, M.; Ganzer, L.; Reitenbach, V. Mathematical modeling of unstable  
transport in underground hydrogen storage. *Environmental Earth Sciences* **2015** (73 (11)), 6891–6898.
- (5) Roy, N.; Molson, J.; Lemieux, J. M.; van Stempvoort, D.; Nowamooz. Three-dimensional numerical simula-  
490 tions of methane gas migration from decommissioned hydrocarbon production wells into shallow aquifers. *Wa-  
ter resources research* **2016** (52 (7)), 5598–5618.
- (6) Osborn, S. G.; Vengosh, A.; Warner, N. R.; Jackson, R. B. Methane contamination of drinking water accompa-  
nying gas-well drilling and hydraulic fracturing. *Proceedings of the National Academy of Sciences* **2011** (108 (20)),  
8172.
- (7) Jenkins, C. R.; Cook, P. J.; Ennis-King, J.; Undershultz, J.; Boreham, C.; Dance, T.; Caritat, P. de; Etheridge, D.  
495 M.; Freifeld, B. M.; Hortle, A.; Kirste, D.; Paterson, L.; Pevzner, R.; Schacht, U.; Sharma, S.; Stalker, L.; Urosevic, M.  
Safe storage and effective monitoring of CO<sub>2</sub> in depleted gas fields. *Proceedings of the National Academy of Sci-  
ences* **2012** (109 (2)), E 35.
- (8) Johnson, G.; Raistrick, M.; Mayer, B.; Shevalier, M.; Taylor, S.; Nightingale, M.; Hutcheon, I. The use of stable  
isotope measurements for monitoring and verification of CO<sub>2</sub> storage. *Energy Procedia* **2009** (1 (1)), 2315–2322.
- 500 (9) Peter, A.; Lamert, H.; Beyer, M.; Hornbruch, G.; Heinrich, B.; Schulz, A.; Geistlinger, H.; Schreiber, B.; Dietrich,  
P.; Werban, U.; Vogt, C.; Richnow, H.-H.; Großmann, J.; Dahmke, A. Investigation of the geochemical impact of

- CO<sub>2</sub> on shallow groundwater: design and implementation of a CO<sub>2</sub> injection test in Northeast Germany. *Environmental Earth Sciences* **2012** (67 (2)), 335–349.
- 505 (10) Cahill, A. G.; Steelman, C. M.; Forde, O.; Kuloyo, O.; Ruff, S. E.; Mayer, B.; Mayer, K. U.; Strous, M.; Ryan, M. C.; Cherry, J. A. Mobility and persistence of methane in groundwater in a controlled-release field experiment. *Nature Geoscience* **2017** (10 (4)), 289–294.
- (11) Gat, J. R.; Mook, W. G.; Meijer, H. *Environmental Isotopes in the Hydrological Cycle*, 2nd ed., 2001.
- (12) Sharp, Z. *Principles of Stable Isotope Geochemistry*, 2nd ed., 2017.
- (13) Fry, B. *Stable Isotope Ecology*; Springer, 2006.
- 510 (14) Hoberman, H. D.; Rittenberg, D. Biological catalysis of the exchange reaction between water and hydrogen. *Journal of Biological Chemistry* **1943** (147 (1)), 211–227.
- (15) Vignais, P. M.; Dimon, B.; Zorin, N. A.; Tomiyama, M.; Colbeau, A. Characterization of the hydrogen-deuterium exchange activities of the energy-transducing HupSL hydrogenase and H<sub>2</sub>-signaling HupUV hydrogenase in *Rhodobacter capsulatus*. *Journal of Bacteriology* **2000** (182 (21)), 5997–6004.
- 515 (16) Löffler, M.; Kümmel, S.; Vogt, C.; Richnow, H.-H. H<sub>2</sub> Kinetic Isotope Fractionation Superimposed by Equilibrium Isotope Fractionation During Hydrogenase Activity of *D. vulgaris* Strain Miyazaki **2019**, *Frontiers in Microbiology* (10 (1545)).
- (17) Farkas, A. The mechanism of the catalytic exchange reaction between deuterium and water. *Transactions of the Faraday Society* **1936** (32), 922–932.
- 520 (18) Clark, I. D.; Fritz, P. *Environmental isotopes in hydrogeology*; CRC press, 1997.
- (19) Wolfsberg, M.; van Hook, W. A.; Paneth, P.; Rebelo, L. P. N. *Isotope effects: in the chemical, geological, and bio sciences*; Springer Science & Business Media, 2009.
- (20) Hoefs, J. *Stable isotope geochemistry*; Springer, 2009.
- (21) Criss, R. E. *Principles of stable isotope distribution*; Oxford University, 1999.
- 525 (22) Prinzhofer, A.; Pernaton, E. Isotopically light methane in natural gas: bacterial imprint or diffusive fractionation? *Chemical Geology* **1997**, *142* (3-4), 193–200.
- (23) Pernaton, E.; A. Prinzhofer, A.; Schneider, F. Reconsideration of methane signature as a criterion for the genesis of natural gas: influence of migration on isotopic signature. *Revue de l'Institut Français du Pétrole*, *1996* (51(5)), 635–651.
- 530 (24) Zhang, T.; Krooss, B. M. Experimental investigation on the carbon isotope fractionation of methane during gas migration by diffusion through sedimentary rocks at elevated temperature and pressure. *Geochimica et Cosmochimica Acta* **2001**, *65* (16), 2723–2742. DOI: 10.1016/S0016-7037(01)00601-9.
- (25) Cahill, A. G.; Marker, P.; Jakobsen, R. Hydrogeochemical and mineralogical effects of sustained CO<sub>2</sub> contamination in a shallow sandy aquifer: A field-scale controlled release experiment. *Water resources research* **2014**, *50* (2), 1735–1755.
- 535 (26) Trautz, R. C.; Pugh, J. D.; Varadharajan, C.; Zheng, L.; Bianchi, M.; Nico, P. S.; Spycher, N. F.; Newell, D. L.; Esposito, R. A.; Wu, Y.; Dafflon, B.; Hubbard, S. S.; Birkholzer, J. T. Effect of dissolved CO<sub>2</sub> on a shallow groundwater system: a controlled release field experiment. *Environmental Science & Technology* **2013**, *47* (1), 298–305. DOI: 10.1021/es301280t. Published Online: Sep. 20, 2012.
- 540 (27) Birkholzer, J. T.; Zhou, Q.; TSANG, C. Large-scale impact of CO<sub>2</sub> storage in deep saline aquifers: A sensitivity study on pressure response in stratified systems. *International Journal of Greenhouse Gas Control* **2009**, *3* (2), 181–194. DOI: 10.1016/j.ijggc.2008.08.002.
- (28) Keller, N.-S.; Hornbruch, G.; Lüders, K.; Werban, U.; Vogt, C.; Kallies, R.; Dahmke, A.; Richnow, H. H. Monitoring of the effects of a temporally limited heat stress on microbial communities in a shallow aquifer. *Science of The Total Environment* **2021**, *781*, 146377.
- 545 (29) Heldt, S.; Wang, B.; Hu, L.; Hornbruch, G.; Lüders, K.; Werban, U.; Bauer, S. Numerical investigation of a high temperature heat injection test. *Journal of Hydrology* **2021**, *597*, 126229.
- (30) Jouanneau, Y.; Kelley, B. C.; Berlier, Y.; Lespinat, P. A.; Vignais, P. M. Continuous monitoring, by mass spectrometry, of H<sub>2</sub> production and recycling in *Rhodospseudomonas capsulata*. *Journal of Bacteriology* **1980** (143 (2)), 628–636.
- 550 (31) Vignais, P. M.; Cournac, L.; Hatchikian, E. C.; Elsen, S.; Serebryakova, L.; Zorin, N.; Dimon, B. Continuous monitoring of the activation and activity of [NiFe]-hydrogenases by membrane-inlet mass spectrometry. *International Journal of Hydrogen Energy* **2002** (27 (11-12)), 1441–1448.

- 555 (32) Vignais, P. M.; Dimon, B.; Zorin, N. A.; Colbeau, A.; Elsen, S. HupUV proteins of *Rhodobacter capsulatus* can bind H<sub>2</sub>: evidence from the H-D exchange reaction. *Journal of Bacteriology* **1997** (179 (1)), 290–292.
- (33) Schulz, A.; Vogt, C.; Lamert, H.; Peter, A.; Heinrich, B.; Dahmke, A.; Richnow, H.-H. Monitoring of a simulated CO<sub>2</sub> leakage in a shallow aquifer using stable carbon isotopes. *Environ. Sci. Technol.* **2012**, *46* (20), 11243–11250. DOI: 10.1021/es3026837. Published Online: Oct. 5, 2012.
- 560 (34) Cahill, A. G.; Parker, B. L.; Mayer, B.; Mayer, K. U.; Cherry, J. A. High resolution spatial and temporal evolution of dissolved gases in groundwater during a controlled natural gas release experiment. *Science of The Total Environment* **2018**, *622*, 1178–1192.
- (35) Clayton, W. S. A field and laboratory investigation of air fingering during air sparging. *Groundwater Monitoring & Remediation* **1998** (18 (3)), 134–145.
- 565 (36) Selker, J. S.; Niemet, M.; Mcduffie, N. G.; Gorelick, S. M.; Parlange, J.-Y. The local geometry of gas injection into saturated homogeneous porous media. *Transport in porous media* **2007** (68 (1)), 107–127.
- (37) Samani, S.; Geistlinger, H. Simulation of channelized gas flow pattern in heterogeneous porous media: A feasibility study of continuum simulation at bench scale. *Vadose Zone Journal* **2019** (18 (1)).
- (38) Geistlinger, H.; Krauss, G.; Lazik, D.; Luckner, L. Direct gas injection into saturated glass beads: Transition from incoherent to coherent gas flow pattern. *Water resources research* **2006** (42 (7)).
- 570 (39) Forde, O. N.; Cahill, A. G.; Mayer, K. U.; Mayer, B.; Simister, R. L.; Finke, N.; Crowe, S. A.; Cherry, J. A.; Parker, B. L. Hydro-biogeochemical impacts of fugitive methane on a shallow unconfined aquifer. *Science of The Total Environment* **2019** (690), 1342–1354.
- 575 (40) Bagnoud, A.; Chourey, K.; Hettich, R. L.; Bruijn, I. de; Andersson, A. F.; Leupin, O. X.; Schwyn, B.; Bernier-Latmani, R. Reconstructing a hydrogen-driven microbial metabolic network in Opalinus Clay rock. *Nature Communications* **2016** (7 (1)), 12770.
- (41) Penfold, W. J. On the Nature of Bacterial Lag. *Journal of Hygiene* **1914** (14 (2)), 215–241.
- (42) Penfold, W. J.; Norris, D. The Relation of Concentration of Food Supply to the Generation-time of Bacteria. *Epidemiology and Infection* **1912** (12 (4)), 527–531.
- 580 (43) Sander, R. Compilation of Henry's law constants (version 4.0) for water as solvent. *Atmos. Chem. Phys.* **2015**, *15* (8), 4399–4981. DOI: 10.5194/acp-15-4399-2015.
- (44) Balcke, G. U.; Meenken, S.; Hofer, C.; Oswald, S. E. Kinetic gas-water transfer and gas accumulation in porous media during pulsed oxygen sparging. *Environmental Science & Technology* **2007**, *41* (12), 4428–4434. DOI: 10.1021/es062890.
- 585 (45) Oswald, S. E.; Griepentrog, M.; Schirmer, M.; Balcke, G. U. Interplay between oxygen demand reactions and kinetic gas-water transfer in porous media. *Water Research* **2008**, *42* (14), 3579–3590. DOI: 10.1016/j.watres.2008.05.035. Published Online: Jul. 11, 2008.
- 590 (46) Heinemann, N.; Alcalde, J.; Miocic, J. M.; Hangx, S.; Kallmeyer, J.; Ostertag-Henning, C.; Hassanpouryouzband, A.; Thaysen, E. M.; Strobel, G. J.; Schmidt-Hattenberger, C.; Edlmann, K.; Wilkinson, M.; Benthams, M.; Haszeldine, R. S.; Carbonell, R.; Rudloff, A. Enabling large-scale hydrogen storage in porous media – the scientific challenges. *Energy & Environmental Science* **2021**, *14* (2), 853–864. DOI: 10.1039/D0EE03536J.
- (47) Bardo, R. D.; Wolfsberg, M. A theoretical calculation of the equilibrium constant for the isotopic exchange reaction between water and hydrogen deuteride. *The Journal of Physical Chemistry* **1976** (80 (10)), 1068–1071.
- (48) Knox, M.; Quay, P. D.; Wilbur, D. Kinetic isotopic fractionation during air-water gas transfer of O<sub>2</sub>, N<sub>2</sub>, CH<sub>4</sub>, and H<sub>2</sub>. *Journal of Geophysical Research: Oceans* **1992**, *97* (C12), 20335–20343.
- 595 (49) Muccitelli, J.; Wen, W.-Y. Solubilities of hydrogen and deuterium gases in water and their isotope fractionation factor. *Journal of Solution Chemistry* **1978** (7 (4)), 257–267.
- (50) Bergman, P. D.; Winter, E. M. Disposal of carbon dioxide in aquifers in the U.S. *Energy Conversion and Management* **1995**, *36* (6-9), 523–526. DOI: 10.1016/0196-8904(95)00058-I.
- 600 (51) Grude, S.; Landrø, M.; Dvorkin, J. Pressure effects caused by CO<sub>2</sub> injection in the Tubåen Fm., the Snøhvit field. *International Journal of Greenhouse Gas Control* **2014**, *27*, 178–187. DOI: 10.1016/j.ijggc.2014.05.013.
- (52) Vignais, P. M.; Billoud, B. Occurrence, classification, and biological function of hydrogenases: an overview. *Chemical Reviews* **2007** (107 (10)), 4206–4272.
- (53) Suess, H. E. Das Gleichgewicht H<sub>2</sub> + HDO  $\rightleftharpoons$  HD + H<sub>2</sub>O und die weiteren Austauschgleichgewichte im System H<sub>2</sub>, D<sub>2</sub> und H<sub>2</sub>O. *Zeitschrift für Naturforschung* **1949** (4 (5)), 328–332.

- 605 (54) Greening, C.; Biswas, A.; Carere, C. R.; Jackson, C. J.; Taylor, M. C.; Stott, M. B.; Cook, G. M.; Morales, S. E. Genomic and metagenomic surveys of hydrogenase distribution indicate H<sub>2</sub> is a widely utilised energy source for microbial growth and survival. *The ISME Journal* **2016**, *10* (3), 761.
- (55) Horibe, Y.; Craig, H. DH fractionation in the system methane-hydrogen-water. *Geochimica et Cosmochimica Acta* **1995** (59 (24)), 5209–5217.
- 610 (56) Schwartz, E.; Friedrich, B. The H<sub>2</sub>-Metabolizing Prokaryotes. In *The Prokaryotes*; pp 496–563.
- (57) Lovley, D. R.; Goodwin, S. Hydrogen concentrations as an indicator of the predominant terminal electron-accepting reactions in aquatic sediments. *Geochimica et Cosmochimica Acta* **1988** (52 (12)), 2993–3003.
- (58) Abram, J. W.; Nedwell, D. B. Hydrogen as a substrate for methanogenesis and sulphate reduction in anaerobic saltmarsh sediment. *Archives of Microbiology* **1978**, 93–97.
- 615 (59) Nedwell, D. B.; Banat, I. M. Hydrogen as an electron donor for sulfate-reducing bacteria in slurries of salt marsh sediment. *Microbial ecology* **1981** (7 (4)), 305–313.
- (60) Hansel, C. M.; Lentini, C. J.; Tang, Y.; Johnston, D. T.; Wankel, S. D.; Jardine, P. M. Dominance of sulfur-fueled iron oxide reduction in low-sulfate freshwater sediments. *The ISME Journal* **2015** (9 (11)), 2400–2412.
- (61) Boone, D. R.; Johnson, R. L.; Liu, Y. Diffusion of the Interspecies Electron Carriers H<sub>2</sub> and Formate in Methanogenic Ecosystems and Its Implications in the Measurement of K<sub>m</sub> for H<sub>2</sub> or Formate Uptake. *Applied and Environmental Microbiology* **1989** (55 (7)), 1735–1741.
- 620 (62) Thiele, J. H.; Zeikus, J. G. Control of Interspecies Electron Flow during Anaerobic Digestion: Significance of Formate Transfer versus Hydrogen Transfer during Syntrophic Methanogenesis in Flocs. *Applied and Environmental Microbiology* **1988** (54 (1)), 20.
- 625 (63) Peters, V.; Janssen, P. H.; Conrad, R. Transient Production of Formate During Chemolithotrophic Growth of Anaerobic Microorganisms on Hydrogen. *Current Microbiology* **1999** (38 (5)), 285–289.
- (64) Blaser, M. B.; Dreisbach, L. K.; Conrad, R. Carbon Isotope Fractionation of 11 Acetogenic Strains Grown on H<sub>2</sub> and CO<sub>2</sub>. *Applied and Environmental Microbiology* **2013** (79 (6)), 1787.